INDIAN JOURNAL OF SCIENCE AND TECHNOLOGY

RESEARCH ARTICLE

# Synthesis, Characterization and Corrosion Inhibition study of N-(4-((4-(pyridin-2-yl) piperazin-1-yl) methyl) phenyl) quinoline-6-carboxamide on Mild Steel under HCl Solution

**S Anbalagan[1,2], M Ravishankar[1]*, S Sivakumar[3], M Sivakumar[3], E Krishna[4]**

**1** Department of Chemistry, Rajah Serfoji Government College, Affiliated to Bharathidhasan University, Thanjur, Tamil Nadu, India
**2** Department of Chemistry, Laxminarayana College of Arts & Science (women), Dharmapuri, Tamil Nadu, India
**3** Department of Chemistry, E. R. K Arts and Science College, Dharmapuri, Tamil Nadu, India
**4** Department of Chemistry, P.S.A Arts and Science College, Dharmapuri, Tamil Nadu, India

OPEN ACCESS

**Received:** 08-12-2022
**Accepted:** 27-01-2023
**Published:** 15-03-2023

**Citation:** Anbalagan S, Ravishankar M, Sivakumar S, Sivakumar M, Krishna E (2023) Synthesis, Characterization and Corrosion Inhibition study of N-(4-((4-(pyridin-2-yl) piperazin-1-yl) methyl) phenyl) quinoline-6-carboxamide on Mild Steel under HCl Solution. Indian Journal of Science and Technology 16(11): 803-815. https://doi.org/10.17485/IJST/v16i11.2364

* **Corresponding author**.

ravishankar1in@yahoo.co.in

**Funding:** None

**Competing Interests:** None

**Copyright:** © 2023 Anbalagan et al. This is an open access article distributed under the terms of the Creative Commons Attribution License, which permits unrestricted use, distribution, and reproduction in any medium, provided the original author and source are credited.

Published By Indian Society for Education and Environment (iSee)

**ISSN**
Print: 0974-6846
Electronic: 0974-5645

## Abstract

**Objectives**: To use the newly synthesized efficient organic corrosion inhibitor N-(4-((4-(pyridin-2-yl) piperazin-1-yl)methyl)phenyl)quinoline-6-carboxamide to carry out on mild steel corrosion inhibition study. **Methods:** N-(4-((4-(pyridin-2-yl)piperazin-1-yl)methyl)phenyl)quinoline-6-carboxamide was synthesized by stirring method under 0$^{o}$C to room temperature at 12 hrs. The synthesized organic inhibitor was characterized by $^{1}$H NMR, $^{13}$C NMR, UV and FTIR spectroscopy. The inhibition effect of organic inhibitor on the mild steel corrosion was investigated with weight loss measurement by gold measuring weighing balance. The inhibitor anchored down on the mild steel surface was analyzed by scanning electron microscopy and Atomic Force Microscopy. **Findings:** The inhibitor shows a better inhibition efficiency of maximum 74.41% in 1N HCl medium. In addition to this adsorption isothermal models were also interpreted to fit the adsorption behavior of the inhibitor compound on mild steel surface. Thus, the result shows the Langmuir adsorption isotherm. As a result, the interactions between inhibitor and mild steel surface have chemisorptions. **Novelty:** The N-(4-((4-(pyridin-2-yl) piperazin-1-yl)methyl)phenyl)quinoline-6-carboxamide shows better corrosion inhibition efficiency (74.41%). In addition, inhibitor and mild steel surface show chemisorptions interaction, which confirms free energy and enthalpy of adsorption.

**Keywords:** Carbaxamide Derivative; Scanning Electronic Microscopy; Atomic Force Microscopy Weight Loss Measurement And NMR

# 1 Introduction

Corrosion causes the major issues in metal related industries because it affects the metallic surface which adversely influence the process efficiency and its economy[1]. The mild steel is not only used in industries but also in households due to low cost and mechanical strength. It is known to be heavily corroded in acidic medium. In various industry applications, acid pickling is a common method for cleaning metallic surfaces and removing the former scaling layer on a substrate although it can cause undesirable corrosion as a side effect[2].

Corrosion inhibitors are the substances which could slow down or prevent the metal corrosion which is of classified as inorganic and organic ones. It is worthy to mention that inorganic inhibitors are not used any longer because they contain harmful heavy metals and their bio-toxicity[3]. Whereas, organic inhibitors are used due to their simple use and effectiveness with small dosage[4]. The effective organic inhibitors may have aromatic rings, unsaturated double bond and heteroatoms as sulfur (S), oxygen (O), and nitrogen (N), can cause the molecules to emit lone electron pairs[5].

The active centers of inhibitor possess the adsorption on the metal surface with the nitrogen and oxygen. These substances have the ability to adhere to metal surfaces, block surface-active sites, and lessen corrosion attack. The corrosion inhibition effectiveness of inhibitors can be related to the quantity of mobile electron pairs present, the nature of free electrons of p orbital, and the density of electrons orbiting nitrogen and oxygen atoms[6]. In comparison to compounds containing simply nitrogen or sulphur, those combining both nitrogen and sulphur can offer greater inhibition[7]. This enhancement corrosion inhibition efficiency of organic inhibitor was also proved some novel works[8,9].

Over the past few decades, several studies have been reported on the corrosion inhibition properties of organic corrosion inhibitors on mild steels under acidic conditions, including Mannich base[10], Schiff base[11], pyridine[12], imidazole[13], etc.

Yeestdev D et al.[14]had reported N-hydroxypyrazine-2-carboxamide as effective inhibitor of mild steel corrosion in hydrochloric acid. Sehmi A et al.[15] investigated the inhibitive effect of newly synthe sized pyrazole carboxamide derivatives on corrosion of brass in HCl medium. Ramachandran A et al.[16]also reported the corrosion inhibition performances of novel heterocyclic carboxamides derivatives on mild steel corrosion in HCl solution.

In view of the aforementioned, the present work was designed towards the investigation of carboxamides with potentially high inhibition efficiencies at relatively low concentrations. The protection performances of some novel quinoline based carboxamide derivatives namely, N-(4-((4-(pyridin-2-yl) piperazin-1-yl)methyl)phenyl)quinoline-6-carboxamide for mild steel in HCl medium are hereby reported. Corrosion inhibition efficiency of mild steel was tested against the mild steel in presence of 1N HCl and was analyzed with the aids of weight loss method and also electrochemical polarization method.

# 2 Methodology

## 2.1 Synthesis of N-(4-((4-(pyridin-2-yl piperazin-1-yl methyl phenyl quinoline-6-carboxamide

Into the 15 mL THF solution of compound 4-{[4-(pyridin-2-yl)piperazin-1-yl]methyl}aniline (1 g, 0.0037 mol), Quinoline-6-carboxylic acid (0.64 g, 0.0037), EDCI.HCl (0.85 g, 0.0044 mol) and HOBt (0.51 g, 0.0037 mol) were added. The reaction mixture was cooled down to 0°C and triethylamine (1.57 mL, 0.011mol) was added. The resulting reaction mixture was allowed and stirred at RT for 12 h. The progress of the reaction was monitored by TLC. The reaction mass was concentrated under reduced pressure and extracted using ethyl acetate (75 mL) and water (1x75 mL). The combined ethyl acetate layer washed with 10% $NaHCO_3$ (1 X 75 mL), brine (1 x 100 mL) and dried over anhydrous $Na_2SO_4$. The resulting solvent was concentrated under reduced pressure to afford titled compound, Off-white solid.

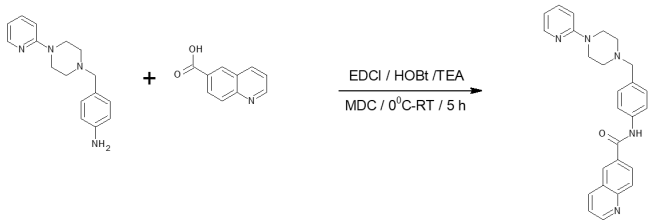


## 2.2 Mild Steel sample preparation

The mild steel specimens (50.00 mm 25.00 mm 1.5.00 mm: length, width, height) were purchased from JSWSTEEL Co., Ltd., (Tamil Nadu, India) with chemical composition (wt%) of 0.098 P; 0.36 Si; 0.53 Mn; 0.20 C; 0.011 S and the remaining Fe. The

mild steel specimen were ground with different emery papers (grade 200, 400, 600 and 800) in order to abrade the surface of mild steel from impurities and for more smoothing for investigation, rinsed with double distilled water, degreased with acetone before use, dried and kept in a desiccator at room temperature.

## 2.3 Inhibitors and solutions

The corrosive solutions of 1 N HCl were prepared by dilution of analytical grade 37% HCl with bidistilled water. The acid solutions for weight loss and electrochemical measurements were used without and with various concentrations of NPPMPQC at room temperature.

## 2.4 Weight Loss Experiment

The weight loss experiments were performed for a duration of 6 h, as per ASTM designation G1-90. The clear and dry specimen was measured for the total surface area with utmost accuracy. The specimen was weighed accurately by a digital balance with a sensitivity of $\pm 0.1$ mg balance. To hold the specimen, a hole with a diameter of 1.5 mm was made near the edge of the specimen. After taking the initial weight and dimensions, the freshly prepared mild steel specimens were suspended into 100 ml beakers containing 90 ml of test solution maintained at room temperature with the aid of glass rods and hooks. To avoid crevice corrosion, the specimens were hanged in the test solution with the help of nylon thread. A blank experiment was also carried out for the comparison purpose. The studies were carried out under varying concentrations inhibitors at room temperature. The experimental conditions were controlled in order to ensure reproducible results. After a definite immersion period, the steel specimen was taken out and washed with running water. The corrosion product was removed mechanically by rubbing with brush on the steel surface. The steel specimen was then dried and the loss in weight was recorded by weighing.

The corrosion rates were determined using the Eq. 2.1.

$$CR = \frac{87.6\,W}{atd} \times 100 \tag{2.1}$$

where W is the weight loss (mg), 'a' represents the exposed area ($cm^2$ ), t refers to the exposed time (h), and 'd' is the stripes density (g. $cm^{-3}$ ).

The percentage inhibition efficiency (% IE) was calculated by using the following equation:

$$\%IE = \frac{CR_o - CR_i}{CR_o} \times 100 \tag{2.2}$$

Where, $CR_o$ is the corrosion rate of mild steel in absence of inhibitor and $CR_i$ is the corrosion rate of mild steel in presence of inhibitor.

## 2.5 Electrochemical measurements

For all corrosion experiments, a traditional 3 electrode device was plugged into the CHI608D electrochemical workstation for the electrochemical experiments. The three-electrode device consisted of a working electrode carbon steel strip, a counter electrode platinum electrode and a saturated calomel electrode as a reference electrode. For electrochemical measurements, a polished working electrode with an exposed area of 1 $cm^2$ (the remainder of the portion was covered by epoxy resin) was used.

The mild steel (working electrode) was dipped in the sample solution for about 30 min for the open circuit potential (OCP) to enter the steady state before performing the electrochemical experiment. The potentiodynamic polarisation curves were obtained within the potential range of +0.2 to -0.2 mV (vs. SCE) with a scan rate of 1.0 mV $s^{-1}$. Electrochemical parameters such as corrosion potential (Ecorr), corrosion current densities (icorr), and Tafel slopes ($\beta$c, $\beta$a) can be derived by extrapolation of the linear Tafel segments of the polarization curves.

Electrochemical impedance study also carried out the same electrochemical workstation with frequency range from 10kHz to 0.01 Hz were fixed with an appropriate equivalent circuit using analyst software and 10 mV amplitude using with open circuit potential all impedance data. The inhibitor efficiency $\eta$% was calculated from charge transfer resistance value obtained from impedance measurement using following relation.

$\eta$% = Rct(inh) – Rct / Rct (inh) X 100 Rct – charge transfer resistance in presence and absence of inhibitor respectively.

The values of double layer were calculated from the following equation Cdl = (mF $X10^{-5}$) 1/n

### 2.6 Steel Surface Analyses

Corroded mild steel surface obtained after immersion in the 1 N HCl solution with and without the optimal concentration of inhibitors was analyzed using scanning electron microscope. AFM was done using a Bruker MULTIMODE instrument. AFM was conducted using a tapping mode and a 2.5 Hz scan rate.

## 3 Results and Discussion

### 3.1 FT-IR characterization of NPPMPQC

The FT-IR spectrum of the synthesized title compound NPPMPQC was recorded by using KBr pellets. The FT-IR spectrum representation of the inhibitor molecule NPPMPQC was shown in Figure 1 (a). The amide group of NPPMPQC was shown as a sharp peak at 3425 and 3340 $cm^{-1}$(NH stretching;) [17]. The characteristic peaks at 1695 and1603 $cm^{-1}$ is assigned to the stretching vibration of C=O and C=C group of the amide linkage and aromatic moity. The C-N stretching vibrations are shown at 1146 (C-N stretch, amide) respectively. The peaks are shown at 816 (CH bend), which are assigned to the bending vibration of CH [18].

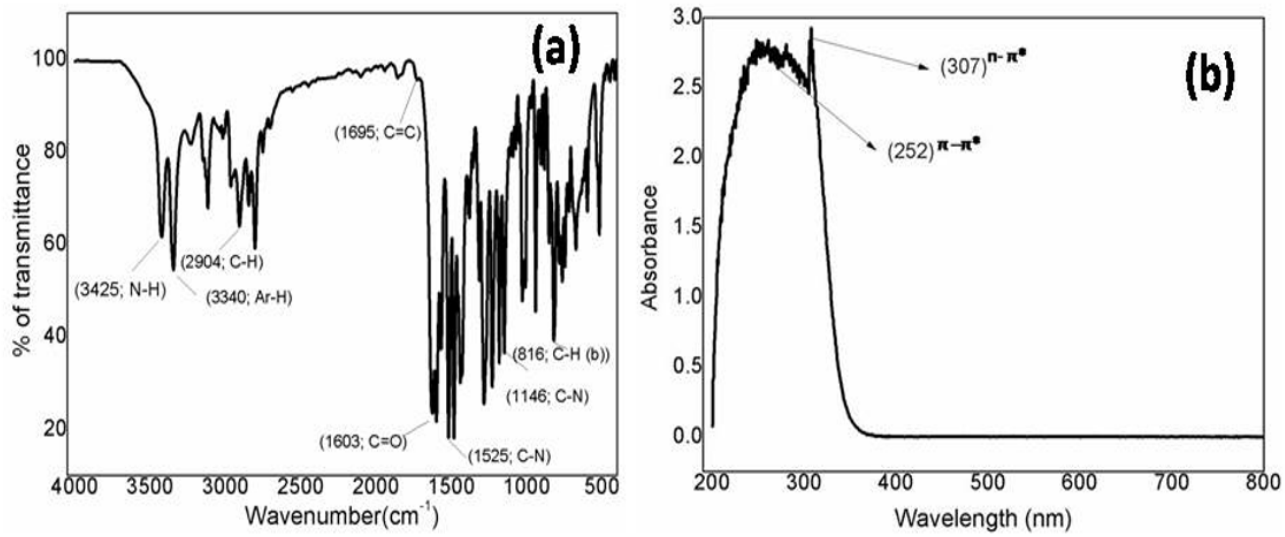


**Fig 1.** (a) FT-IR spectrum of NPPMPQC (b) UV-visible spectrum of NPPMPQC

### 3.2 NMR spectral analysis

NMR spectrum clearly interpreted the structure of organic inhibitors which is shown in Figure 2. The $CH_2$ group of piprazene moiety that was detected at 2.6 ppm (triplet) was verified by the $^1H$ NMR. The NPPMPQC contains aromatic protons were seen in the range of 7.18 to 8.95 ppm [19]. Singlet signals of the active methylene group, which served as a linker between the phenyl and the tertiary nitrogen of piperazine, at roughly 3.5 ppm and their integration for two protons in each case, are used to demonstrate the formation of NPPMPQC.

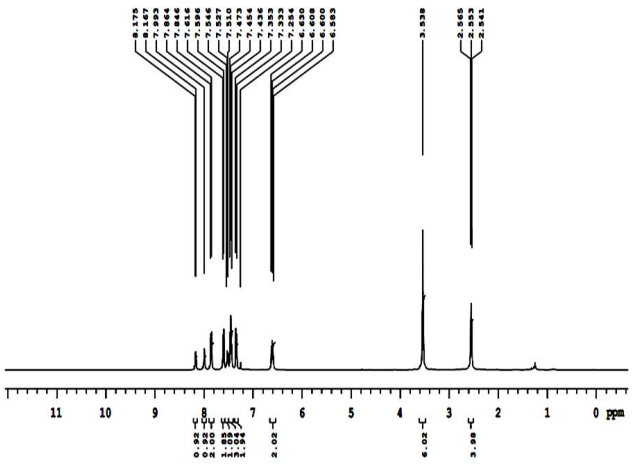

**Fig 2.** $^{1}$H NMR spectrum of NPPMPQC

The chemical shift of amide carbonyl carbons (C=O) are shown in the $^{13}$C-NMR spectra of the product produced at 165.77 ppm, and are caused by the benzothiazol and quinoline moieties, respectively (Figure 3). The aromatic C-N groups of the quinoline moiety are ascribed to the chemical shift values found at 159 (Figure 3). Peaks in the 147 ppm to 120.01 ppm range that are attributed to the aromatic carbons of the phenyl and Quinoline.

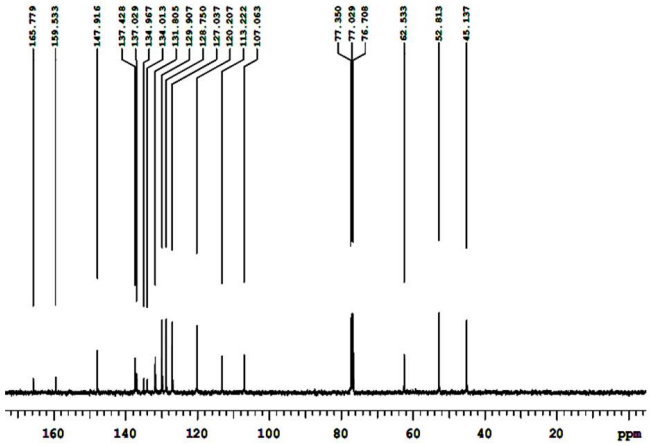

**Fig 3.** $^{13}$C NMR spectrum of NPPMPQC

## 3.3 UV-visible spectrum of NPPMPQC

UV-visible spectroscopy analyses were performed to obtain more information on the nature electronic excitation of organic molecules. Figure 3 shows the UV-visible spectrum of NPPMPQC. The NPPMPQC inhibitors show absorption bands observed between 252 nm and 307 nm, which are attributed to $\pi-\pi^*$ and n$-\pi^*$ respectively. This electronic transition indicates, the NPPMPQC contains C=O and C=C bonding [20].

**Table 1.** Calculated values of corrosion rate (mmpy) and inhibition efficiency (% IE) for mild steel in 1M HCl in the absence and presence of NPPMPQC from weight loss measurement

| S.No | Inhibitor concentration (ppm) | Weight loss (mg) | | | Corrosion rate (mmpy) | Surface coverage (q) | Inhibitor efficiency (%) |
|---|---|---|---|---|---|---|---|
| | | Initial | Final | Loss of Weight | | | |
| 1 | 0 | 4.1223 | 3.7002 | 0.4221 | 0.0087 | - | - |
| 2 | 20 | 4.1433 | 3.9002 | 0.2431 | 0.0050 | 0.4137 | 41.37 |
| 3 | 40 | 4.1533 | 3.9510 | 0.2023 | 0.0042 | 0.5172 | 51.72 |
| 4 | 60 | 4.2000 | 4.0356 | 0.1644 | 0.0034 | 0.6091 | 60.91 |
| 5 | 80 | 4.1543 | 4.0487 | 0.1056 | 0.0022 | 0.7471 | 74.71 |
| 6 | 100 | 4.1245 | 3.9945 | 0.1300 | 0.0027 | 0.6896 | 68.96 |

## 3.4 Corrosion inhibition studies

### *3.4.1 Weight loss measurement*

Weight loss measurement technique was performed on mild steel in the room temperature in 1 N HCl for NPPMPQC for 6 h of immersion. The suitable formulae, used for the calculation of corrosion rate (CR), inhibition efficiency (IE) and surface coverage (SC) results are tabulated.

Variations in $C_R$ with the change in concentration are depicted in Figure 4 (a). $C_R$ decreased considerably with increase in concentration of NPPMPQC, but the extent of inhibition offered by NPPMPQC. The increase in inhibition efficiencies with increase in concentration is due to increased surface coverage caused by adsorption of inhibitors. The maximum inhibition efficiencies exhibited were 74.41% in presence of 80 ppm NPPMPQC (Figure 4 (b)). When increased the inhibitor concentration above 80 ppm, might decrease the inhibiting efficiency due to desorption of inhibitor on the mild steel surface. The protective property of corboximide may be due to the interaction between -electrons and lone pair of electrons present on oxygen and nitrogen with charged steel surface [21]. Presence of carbonyl group attached NH groups donating two electrons contributes to the inhibition on mild steel surface and aromatic moity group also enhances the inhibition efficiency because the electron density is more towards aromatic moity group. As a result, the net negative charge developed on the aromatic group results in good inhibition effect [17]. In the presence of hydrochloric acid, protonation can occur on carbonyl oxygen atom or nitrogen atom. When the protonation occurs, solubility of the inhibitor increases. This has positive effect on inhibition efficiency. The general trend reported in the inhibition efficiencies of molecules containing heteroatoms is in the order O<N<S<P. The higher inhibition efficiency shown by NPPMPQC is due to better electron donating capacity due to the presence of nitrogen and oxygen atom cover the mild steel surface (Figure 4 (c)).

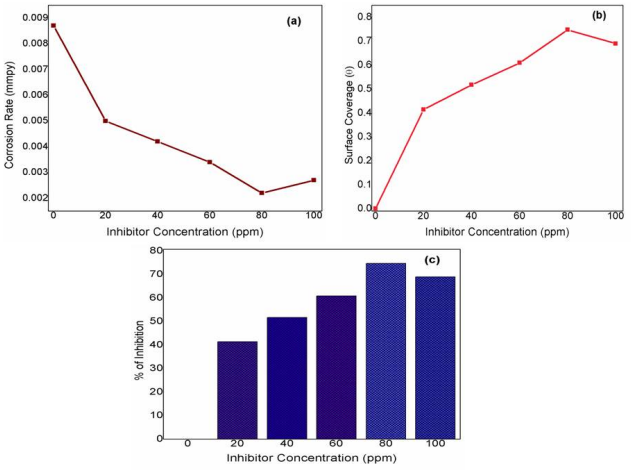


**Fig 4.** (a) Corrosion rate of NPPMPQC on mild steel (b) Corrosion inhibition efficiency of NPPMPQC on mild steel (c) Surface coverage of NPPMPQC on mild steel

### *3.4.2 Electrochemical Studies*

3.4.2.1 Electrochemical Impedance Spectroscopy. The inhibition efficiency of the inhibitor was investigated by Electrochemical Impedance Spectroscopy (EIS), which is also a good appropriate technique. This technique clearly explains the adsorptive nature of the NPPMPQC inhibitor over the mild steel surface in 1N HCl medium (Figure 5). For diverse corrosion system features of EIS Spectra had been validated based totally on their charge transfer control, diffusion control of inhibitor. From Nyquist plot (EIS data), the mechanism of corrosion may be diagnosed. An electrochemical interface which in term referred as electrical features may be interpreted the usage of EIS information [22]. In homogeneity of the surface and roughness of the electrodes recurrently refers to frequency dispersion. The depressed semicircle with the center under beneath the actual axis of Nyquist plot presentation the characteristic for solid electrodes [23]. Nyquist plots for interface of mild steel electrode and electrolyte in non-existence and the existence of inhibitor at various concentrations shown in Figure 5. Impedance parameters were exemplified in Table 2. The presence of the N-H group and phenyl group in the inhibitor compound shows a better efficacy on prevention of mild steel material.

**Table 2.** Impedance parameters of mild steel electrode soaked in 1N HCl without and with inhibitor atroom temperature

| S.No | Inhibitor concentration (ppm) | Rct(ohm $cm^2$ ) | Cdl(mF $X10^{-5}$ ) | Inhibition Efficiency (%) |
|---|---|---|---|---|
| 1 | Blank | 21.48 | 89.23 | - |
| 2 | 20 | 52.48 | 74.34 | 20.2 |
| 3 | 40 | 79.32 | 35.40 | 25.66 |
| 4 | 80 | 95.90 | 29.40 | 70.34 |

The fitted solid lines in Figure 5 using the open electric circuit of Figure 6 are in accordance with EIS test data, indicating that the equivalent circuit can be used to fit the experimental data. Rs is the solution resistance, Rct is the charge transfer resistance and Cdl represents the double layer charge, of the adsorption characteristics of inhibitor on the electrode surface.

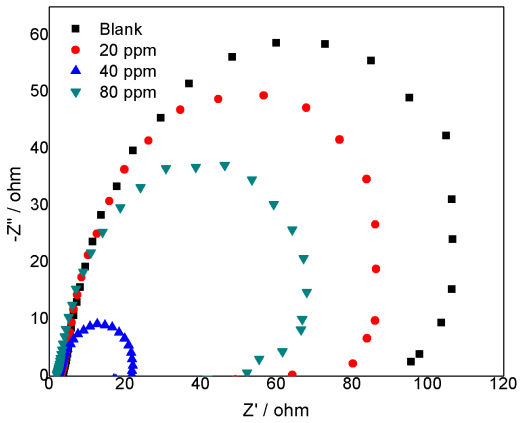


**Fig 5.** Impedance curves of mild steel electrode soaked in 1N HCl in the absence and presence of the inhibitor at 303K

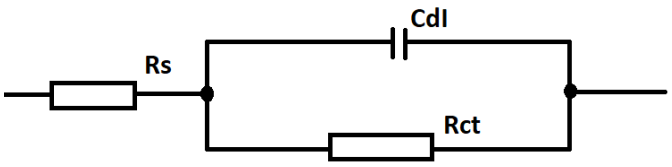


**Fig 6.** Open circuit model used to fit impedance spectra

The electrochemical Tafel polarisation curves for mild steel without and with the addition of different concentrations of NPPMPQC in 1N HCl at 303 K are shown in Figure 7. The graph of current against potential was plotted at the given potential

range at the scan rate of 0.01 mV/s. Table 3 consists of corrosion parameters viz., corrosion potential (Ecorr), corrosion current density (icorr), Corrosion rate ($v$) and inhibition efficiency ($\eta$p). The inhibition efficiency of NPPMPQC for mild steel in 1N HCl is computed by the following expression [24], The inhibition efficiency (IE, %) from potentiodynamic polarization was calculated using the following equation:

$$\%IE = \frac{I0 - I'}{I0} \times 100 \tag{3.3}$$

where $I_0$ and I' are the corrosion current density without and with the inhibitor, respectively. The results show that with increasing NPPMPQC concentrations, the corrosion rate is gradually decreasing. This is due to the accumulation of NPPMPQC by adsorption from the bulk solution onto the metal surface.

**Table 3.** Corrosion parameterslike corrosion potential (Ecorr), corrosion current density (icorr), Corrosion rate ($v$) and inhibition efficiency ($\eta$p)

| S.No | Inhibitor Concentration (ppm) | $E_{corr}$ (V) | icorr (A) (A) | Corrosion rate (mm/year) | Inhibition Efficiency (%) |
|---|---|---|---|---|---|
| 1 | 0 | -0.36477 | 0.000336 | 3.9092 | - |
| 2 | 20 | -0.33947 | 0.000273 | 3.1736 | 18.81 |
| 3 | 40 | -0.37184 | 0.00027 | 3.141 | 19.65 |
| 4 | 60 | -0.37111 | 0.000256 | 2.9798 | 23.77 |
| 5 | 80 | -0.35454 | 0.000117 | 1.3614 | 65.17 |
| 6 | 100 | -0.35254 | 0.000146 | 1.7009 | 56.48 |

The adsorbed molecules on metal surfaces block the corrosion sites, which reduce the rate of corrosion. It is also stated that the corrosion rate (v) decreases with the increasing concentration of inhibitor in 1N HCl. From the above data, it is concluded that the corrosion inhibition efficiency also increases for mild steel in 1N HCl solution as the concentration of the inhibitor increases. Therefore, NPPMPQC exhibits high inhibition efficiency, but due to the destruction of adsorbed layers over the mild steel surfaces, inhibition efficiency decreases with the increasing inhibitor concentration.

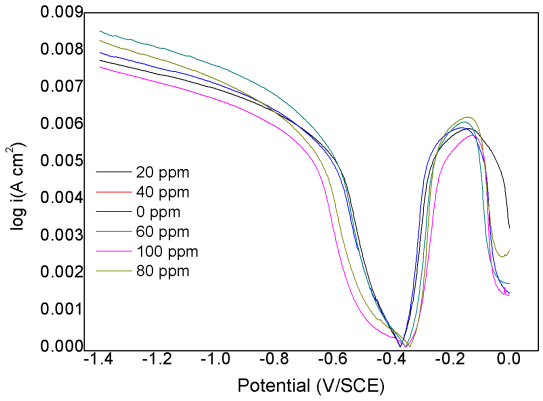


**Fig 7.** Electrochemical Tafel polarisation curves for mild steel without and with the addition of different concentrations of NPPMPQC in 1M HCl

### *3.4.3 Corrosion Mechanism*

Details on the interaction between inhibitor molecules and the mild steel surface are needed to characterize the inhibition mechanism which is shown in Figure 8. In an acidic solution, mild steel is positively charged, and the inhibitor molecules are either neutral or protonated. As stated earlier, it is difficult to understand how inhibitor molecules adsorb; they may do so in several ways. As a result of a synergistic interaction with pre-adsorbed $Cl^-$, the protonated sites of inhibitor molecules leap to adsorb on the metal surface.

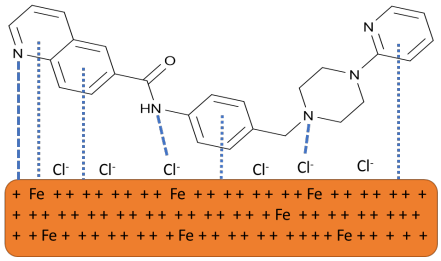


**Fig 8.** Corrosion inhibition mechanism of NPPMPQC on mild steel

Inhibitor molecules that are positively charged begin competing with $H^+$ for electrons on the MS surface and, after liberating $H_2$,[16] transition back to the neutral state where they are ready to accept empty d orbitals of iron atoms. The iron's d orbital's excess negative charges can be transferred to the empty (antibonding) of inhibitor molecules, accumulating extra negative charges on the mild steel surface.

### *3.4.4 Adsorption Isotherm*

The communal effects between inhibitors and the metallic surface are able to be examined over the adsorption isotherm since inhibitors normally adsorb upon the metal/solution surface[23].

Among various adsorption isotherms (Langmuir, Frumkin, Temkin), Langmuir adsorption isotherm displays the finest explanation for the adsorption behavior of the investigated inhibitors since the correlation coefficient ($R^2$) were close to 1. Langmuir isotherm and corresponding adsorption thermodynamics parameters can be conveyed by the following equation 3.4.

$$\frac{C}{\theta} = \frac{1}{K_{abs}} + C$$

$$K_{abs} = \frac{1}{55.5} exp\left(\frac{-\triangle G^o_{ads}}{RT}\right) \tag{3.4}$$

where C shows the concentration of inhibitors; $\theta$ stands for surface coverage, whose value has been calculated by weight loss test; $K_{ads}$ is the adsorptive equilibrium constant; T stands for the thermodynamic temperature; R is the universal gas constant and 55.5 represents the molar concentration of water in solution. Figure 9 shows the plot of C/$\theta$ against inhibitor concentration C at 303 K and the expected linear relationship is obtained for compounds with excellent correlation coefficents ($R^2$), confirming the validity of this approach.

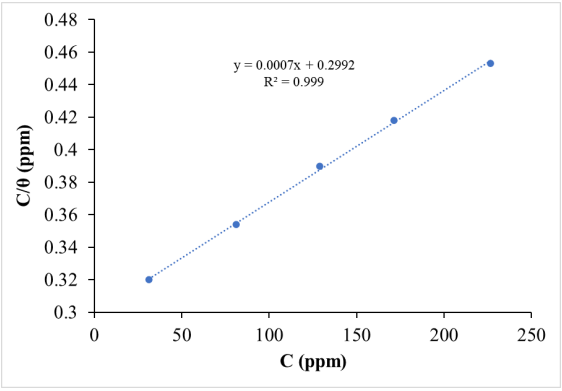


**Fig 9.** Adsorption isotherm of NPPMPQC on mild steel

The slopes of the straight lines are even, signifying that adsorbed inhibitor molecules form monolayer on the mild steel surface and there is no interface among the adsorbed inhibitor molecules. From the DG values less than -20 kJ/mol means

physical adsorption (intermolecular forces between adsorbent and adsorbate) and values more than -40 kJ/mol specifies that a chemisorption process (the formation of coordination bonds between the inhibitor molecules and iron atoms of steel surface) [25]. The calculated $\Delta G^0_{ads}$ values such as -38.3, -39.5, -40.3 and -37.9 obtained in the temperatures 303, 313, 323 and 333 respectively. Hence, this adsorption isotherm model exhibits the chemisorptions phenomenon.

The Gibbs-Helmholtz equation measures the enthalpy of adsorption ($\Delta H^0_{ads}$) as follows [24].

$$\left(\frac{\triangle G/T}{\triangle T}\right)P = \frac{H}{T2} \tag{3.5}$$

The reordered form of the above equation is as follows. Figure 10 describes a plot of $\Delta G^0_{ads}$/T against 1000/T with a slope value equal to $\Delta H^0_{ads}$ (Table 4). Generally, the values of $\Delta H^0_{ads}$ reach -100 kJ/mol include the process of chemisorption [26,27]. In this work, we find that the magnitude of adsorption enthalpy is -107 kJ/mol and its indicates that the inhibitor has been chemically adsorbed on mild steel surfaces.

**Table 4.** lot of $\Delta G^0_{ads}$/T against 1000/T with 80 ppm of NPPMPQC

| S.No | Temperature | $\Delta G^o_{ads}$ (KJ mol$^{-1}$ ) | $\Delta G^o_{ads}$ /T | $\Delta H^o_{ads}$(KJ mol$^{-1}$ ) |
|---|---|---|---|---|
| 1 | 303 | -38.3 | -0.1148 | -107 |
| 2 | 313 | -39.5 | -0.1202 | |
| 3 | 323 | -40.3 | -0.1237 | |
| 4 | 333 | -37.9 | -0.1274 | |

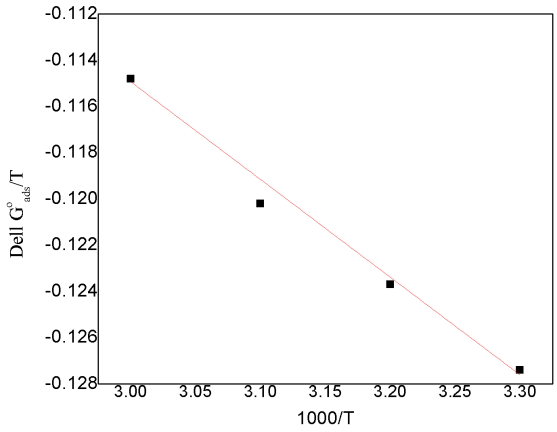


**Fig 10.** Enthalpy of adsorption (a plot of $\Delta G^0_{ads}$/T against 1000/T) (80 ppm inhibitor concentration)

### *3.4.5 Surface properties analysis*

Figure 11 (a) the polished mild steel surface 12 (b) mild steel immersed in 1M HCl 12(c) mild steel surfaces immersed in 1M HCl with 20 ppm NPPMPQC, Figure 11 (d) 80 ppm of NPPMPQC adhered mild steel surface in 1M HCl

The results of the semi-micrograph show that when the MS plate is dipped in a blank solution, more pits occur while examining the plates dipped in the solution. There are no apparent corrosion holes found and portions of the cleaned-out trench is still discernible [28]. As a result, they show that the addition of NPPMPQC to a solution of 1N HCl acid can effectively suppress the corrosion of mild steel by correlating the SEM images of Figure 12 (a), and 13(b). The AFM picture further confirms that the surface morphology of mild steel was changed when an inhibitor was added to an acid solution due to the creation of an adsorbed protective layer [4], which can be explained by a decrease in surface roughness mild steel.

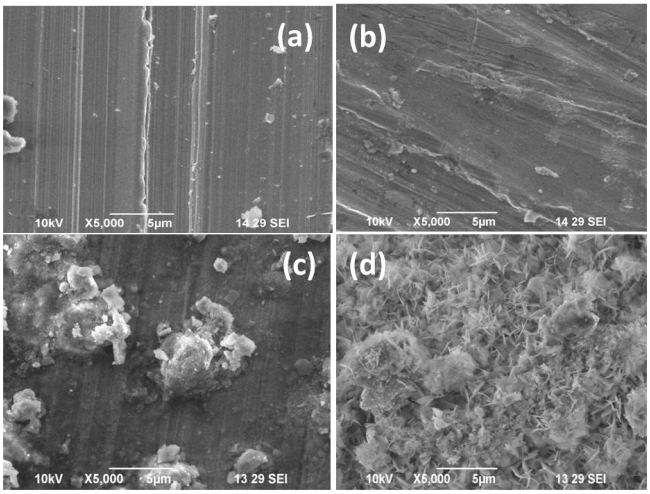


**Fig 11.** (a) The polished mild steel surface 11(b) mild steel immersed in 1M HCl 11(c) mild steelsurfaces immersed in 1M HCl with 20 ppm NPPMPQC, Figure 11(d) 80 ppm of NPPMPQC adhered mild steel surface in 1M HCl

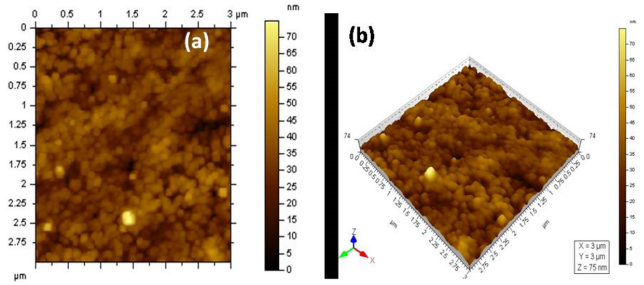


**Fig 12.** AFM images of NPPMPQC inhibitor coated on mild steel surface

## 4 Conclusion

The experimental studies were performed to evaluate the new compound N-(4-((4-(pyridin-2-yl)piperazin-1-yl)methyl)phenyl)quinoline-6-carboxamide (NPPMPQC) as a corrosion inhibitor for the mild steel in 1 N HCl.

The following are some concluded findings:

- The NPPMPQC inhibitor chemical structure could be confirmed by using FTIR, UV and NMR studies.
- Chemical (weight loss) method was employed for the measuring the corrosion inhibition and also electrochemical polarization method.
- NPPMPQC revealed potential as a corrosion inhibitor, and the results indicated that the performance of corrosion was dependent on its concentration.
- The weight loss measurements exploiting 80 ppm of NPPMPQC resulted in inhibition performance of 74.41%.
- Tafel polarization data showed that NPPMPQC act as good inhibitor which predominantly suppressed the anodic reaction. EIS measurements revealed that the inhibitor molecules instead of water molecules on steel surface took effect by adsorption at the electrode/solution interface.
- The thermodynamic data of adsoption indicated that the adsorption of NPPMPQC on the surface of mild steel was a chemical process and obeyed the isotherm of the Langmuir model.
- AFM results and surface analyses (SEM) suggested that the mechanism of corrosion inhibition was through the formation of a stable protective film on the metal surface, and accordingly inhibition performance increased with an increase in the inhibitor concentration due to the better surface coverage.

## Acknowledgement

The authors gratefully acknowledge the support received for this research work from the Department of Chemistry, Rajah Serfoji Government College, Affiliated to Bharathidhasan University, Thanjur, Tamilnadu, India.

## References

1) Omran MA, Fawzy M, Mahmoud AED, Abdullatef OA. Optimization of mild steel corrosion inhibition by water hyacinth and common reed extracts in acid media using factorial experimental design. *Green Chemistry Letters and Reviews*. 2022;15(1):216–232. Available from: https://doi.org/10.1080/17518253.2022.2032844.
2) Salmasifar A, Edraki M, Alibakhshi E, Ramezanzadeh B, Bahlakeh G. Combined electrochemical/surface investigations and computer modeling of the aquatic Artichoke extract molecules corrosion inhibition properties on the mild steel surface immersed in the acidic medium. *Journal of Molecular Liquids*. 2021;327:114856. Available from: https://doi.org/10.1016/j.molliq.2020.114856.
3) Kumar H, Yadav V, Anu, Saha SK, Kang N. Adsorption and inhibition mechanism of efficient and environment friendly corrosion inhibitor for mild steel: Experimental and theoretical study. *Journal of Molecular Liquids*. 2021;338:116634. Available from: https://doi.org/10.1016/j.molliq.2021.116634.
4) Wu Y, Guo L, Tan B, Li W, Zhang F, Zheng X. 5-Mercapto-1-phenyltetrazole as a high-efficiency corrosion inhibitor for Q235 steel in acidic environment. *Journal of Molecular Liquids*. 2021;325:115132. Available from: https://doi.org/10.1016/j.molliq.2020.115132.
5) Sheetal, Batra R, Singh AK, Singh M, Thakur S, Pani B, et al. Advancement of corrosion inhibitor system through N-heterocyclic compounds: a review. *Corrosion Engineering, Science and Technology*. 2023;58(1):73–101. Available from: https://doi.org/10.1080/1478422X.2022.2137979.
6) Ashassi-Sorkhabi H, Kazempour A, Frouzat Z. Superior potentials of hydrazone Schiff bases for efficient corrosion protection of mild steel in 1.0 M HCl. *Journal of Adhesion Science and Technology*. 2021;35(2):164–184. Available from: https://doi.org/10.1080/01694243.2020.1794357.
7) Kaabi I, Douadi T, Daoud D, Issaadi S, Sibous L, Chafaa S. Synthesis, characterization and anti-corrosion properties of two new Schiff bases derived from diamino diphenyl ether on carbon steel X48 in 1M HCl. *Journal of Adhesion Science and Technology*. 2021;35(6):559–589. Available from: https://doi.org/10.1080/01694243.2020.1816777.
8) Alamiery AA. Investigations on Corrosion Inhibitory Effect of Newly Quinoline Derivative on Mild Steel in HCl Solution Complemented with Antibacterial Studies. *Biointerface Research in Applied Chemistry*. 2022;12(2):1561–1568. Available from: https://doi.org/10.33263/BRIAC122.15611568.
9) Al-Amiery AA, Shaker LM. Corrosion inhibition of mild steel using novel pyridine derivative in 1 M hydrochloric acid. *Koroze a ochrana materialu*. 2020;64(2):59–64. Available from: https://doi.org/10.2478/kom-2020-0009.
10) Chen Y, Chen Z, Zhuo YZ. Newly Synthesized Morpholinyl Mannich Bases as Corrosion Inhibitors for N80 Steel in Acid Environment. *Materials*. 2022;15(12):4218. Available from: https://doi.org/10.3390/ma15124218.
11) Sami MB, Munakhethier A, Khudhair M, M, Khalid W, Mahdi A, et al. Corrosion Inhibition of Mild Steel in Hydrochloric Acid Environment Using Terephthaldehyde Based on Schiff Base: Gravimetric, Thermodynamic, and Computational Studies. *Molecules*. 2022;27. Available from: https://doi.org/10.3390/molecules27154857.
12) Alrebh A, Rammal MB, Omanovic S. A pyridine derivative 2-(2-Methylaminoethyl)pyridine (MAEP) as a 'green' corrosion inhibitor for low-carbon steel in hydrochloric acid media. *Journal of Molecular Structure*. 2021;1238:130333. Available from: https://doi.org/10.1016/j.molstruc.2021.130333.
13) Mishra A, Aslam J, Verma C, Quraishi MA, Ebenso EE. Imidazoles as highly effective heterocyclic corrosion inhibitors for metals and alloys in aqueous electrolytes: A review. *Journal of the Taiwan Institute of Chemical Engineers*. 2020;114:341–358. Available from: https://doi.org/10.1016/j.jtice.2020.08.034.
14) Yeestdev D, Dakeshwar KV, Elyor B, Rajesh H, Mamtatripathi OD, Kumar V, et al. N-hydroxypyrazine-2-carboxamide as a new and green corrosion inhibitor for mild steel in acidic medium: experimental, surface morphological and theoretical approach. *Journal of Adhesion Science and Technology*. 2022. Available from: https://doi.org/10.1080/01694243.2022.2068884.
15) Sehmi A, Ouici HB, Guendouzi A, Ferhat M, Benali O, Boudjellal F. Corrosion Inhibition of Mild Steel by newly Synthesized Pyrazole Carboxamide Derivatives in HCl Acid Medium: Experimental and Theoretical Studies. *Journal of The Electrochemical Society*. 2020;167(15):155508. Available from: https://doi.org/10.1149/1945-7111/abab25.
16) Ramachandran A, Anitha P, Gnanavel S. Structural and electronic impacts on corrosion inhibition activity of novel heterocyclic carboxamides derivatives on mild steel in 1 M HCl environment: Experimental and theoretical approaches. *Journal of Molecular Liquids*. 2022;359:119218. Available from: https://doi.org/10.1016/j.molliq.2022.119218.
17) Ranjith PK, Ignatious A, Panicker CY, Sureshkumar B, Armakovic S, Armakovic SJ, et al. Spectroscopic investigations, DFT calculations, molecular docking and MD simulations of 3-[(4-Carboxyphenyl) carbamoyl]-4-hydroxy-2-oxo-1, 2-dihydroxy quinoline-6-carboxylic acid. *Journal of Molecular Structure*. 2022;1264(15):133315. Available from: https://doi.org/10.1016/j.molstruc.2022.133315.
18) Yuhaoc Z, Yaowen Z. Newly Synthesized MorpholinylMannich Bases as Corrosion Inhibitors for N80 Steel in Acid. *Environment*. 2022;15:4218–4219. Available from: https://doi.org/10.3390/ma15124218.
19) Bhawna C, Singh AK, Sanjeeve T, Balaram P, Hassane L, Ill-Min C, et al. Comparative Investigation of Corrosion-Mitigating Behavior of Thiadiazole-Derived Bis-Schiff Bases for Mild Steel in Acid Medium:Experimental, Theoretical, and Surface Study. *ACS Omega* . 2020;5:13503. Available from: https://doi.org/10.1021/acsomega.9b04274.
20) Senthilkumar G, Umarani C, Ramachandran A. Investigation on corrosion inhibition effect of N-[4-(1,3-benzo[d]thiazol-2-ylcarbamoyl)phenyl]quinoline-6-carboxamide as a novel organic inhibitor on mild steel in 1N HCl at different temperatures: Experimental and theoretical study. *Journal of the Indian Chemical Society*. 2021;98(6):100079. Available from: https://doi.org/10.1016/j.jics.2021.100079.
21) Zhang X, Zhang M, Zhang Z, Li Q, Lv R, Wu W. Bis-Mannich bases as effective corrosion inhibitors for N80 steel in 15% HCl medium. *Journal of Molecular Liquids*. 2022;347:117957. Available from: https://doi.org/10.1016/j.molliq.2021.117957.
22) Senthilkumar G, Umarani C, Ramachandran A. Synthesis of Novel corrosion Inhibitor N- (1,3-Benzothiazole-2yl) 4-Aminobenzamide in 1 Hydrochloric acid Medium. *Asian Journal of chemistry*. 2021;33(3):622–626. Available from: https://doi.org/10.14233/ajchem.2021.23042.
23) Praveen BM, Prasanna BM, Mallikarjuna NM, Jagadeesh MR, Hebbar N, Rashmi D. Investigation of anticorrosive behaviour of novel tert-butyl 4-[(4-methyl phenyl) carbonyl] piperazine-1-carboxylate for carbon steel in 1M HCl. *Heliyon*. 2021;7(2):e06090. Available from: https://doi.org/10.1016/j.heliyon.2021.e06090.
24) Kumarm R, Mahendray, Obot I. Electrochemical and computational investigation of adsorption and corrosion inhibition behaviour of 2-aminobenzohydrazide derivatives at mild steel surface in 15% HCl. *Materials Chemistry and Physics*. 2022;290:126666. Available from: https://doi.

org/10.1016/j.matchemphys.2022.126666.
25) Praveen BM, Alhadhrami A, Prasanna BM, Hebbar N, Prabhu R. Anti-Corrosion Behavior of Olmesartan for Soft-Cast Steel in 1 mol dm−3 HCl. *Coatings*. 2021;11(8):965. Available from: https://doi.org/10.3390/coatings11080965.
26) Guruprasad AM, Sachin HP, Swetha GA, Prasanna BM. Corrosion inhibition of zinc in 0.1 M hydrochloric acid medium with clotrimazole: Experimental, theoretical and quantum studies. *Surfaces and Interfaces*. 2020;19:100478. Available from: https://doi.org/10.1016/j.surfin.2020.100478.
27) Prasanna BM, Praveen BM, Hebbar NBM, Pavithra MK, Manjunatha TS, Malladi RS. Theoretical and experimental approach of inhibition effect by sulfamethoxazole on mild steel corrosion in 1-M HCl. *Surface and Interface Analysis*. 2018;50(8):779–789. Available from: https://doi.org/10.1002/sia.6457.
28) Praveen BM, Prasanna BM, Mallikarjuna NM, Jagadeesh MR, Hebbar N, Rashmi D. Investigation of anticorrosive behaviour of novel tert-butyl 4-[(4-methyl phenyl) carbonyl] piperazine-1-carboxylate for carbon steel in 1M HCl. *Heliyon*. 2021;7(2):e06090. Available from: https://doi.org/10.1016/j.heliyon.2021.e06090.